Longitudinal Structure Function Measurements from HERA[1]

Vladimir Chekelian (Shekelyan)
Max-Planck-Institute für Physik
Föhringer Ring 6, 80805 Munich, Germany

Abstract

Measurements of the longitudinal structure function F_L at the ep collider HERA are presented. They are derived from inclusive deep inelastic neutral current e^+p scattering cross section measurements based on data collected in 2007 with the H1 and ZEUS detectors at a positron beam energy of 27.5 GeV and proton beam energies of $920, 575$ and 460 GeV. Employing the energy dependence of the cross sections, $F_L(x, Q^2)$ is measured in the range of negative four-momentum transfer squared $12 \leq Q^2 \leq 800$ GeV^2 and low Bjorken-x $0.00028 \leq x \leq 0.0353$. The measured longitudinal structure function is compared with higher order QCD predictions.

1 Introduction

In the past 15 years, the HERA experiments H1 and ZEUS have extended the knowledge of the proton structure by two orders of magnitude towards high negative four-momentum transfer squared, Q^2, and to small Bjorken-x. At the end of the HERA operation in 2007, dedicated e^+p data were collected with lower proton beam energy which allow to measure the longitudinal component of the proton structure. This measurement is directly sensitive to the gluon contribution in the proton. It is essential for completion of the deep inelastic scattering (DIS) program at HERA and for checks of the underlying perturbative Quantum Chromodynamics (QCD) framework used to determine parton distribution functions (PDFs).

The DIS neutral current (NC) ep scattering cross section at low Q^2 can be written in reduced form as

$$\sigma_r(x, Q^2, y) = \frac{d^2\sigma}{dxdQ^2} \cdot \frac{Q^4 x}{2\pi\alpha^2[1 + (1-y)^2]} = F_2(x, Q^2) - \frac{y^2}{1 + (1-y)^2} \cdot F_L(x, Q^2) \ . \quad (1)$$

---

[1] Invited talk at the XXVIII International Symposium on Physics in Collision, Perugia, Italy, 25-28 June 2008.

Here, α denotes the fine structure constant, x is the Bjorken scaling variable and y is the inelasticity of the scattering process related to Q^2 and x by $y = Q^2/sx$, where s is the centre-of-mass energy squared of the incoming electron and proton.

The cross section is determined by two independent structure functions, F_2 and F_L. They are related to the γ^*p interaction cross sections of longitudinally and transversely polarised virtual photons, σ_L and σ_T, according to $F_2 \propto (\sigma_L + \sigma_T)$ and $F_L \propto \sigma_L$, therefore $0 \leq F_L \leq F_2$. F_2 is the sum of the quark and anti-quark x distributions weighted by the electric charges of quarks squared and contains the dominant contribution to the cross section. In the Quark Parton Model the value of the longitudinal structure function F_L is zero, whereas in QCD it differs from zero due to gluon and (anti)quarks emissions. At low x the gluon contribution to F_L exceeds the quark contribution and F_L is a direct measure of the gluon x distribution.

The longitudinal structure function, or equivalently $R = \sigma_L/\sigma_T = F_L/(F_2 - F_L)$, was measured previously in fixed target experiments and found to be small at large $x \geq 0.2$, confirming the spin $1/2$ nature of the constituent quarks in the proton. From next-to-leading order (NLO) and NNLO [1] QCD analyses of the inclusive DIS cross section data [2, 3, 4], and from experimental F_L determinations by H1 [5, 6], which used assumptions on the behaviour of F_2, the longitudinal structure function F_L at low x is expected to be significantly larger than zero. A direct, free from theoretical assumptions, measurement of F_L at HERA, and its comparison with predictions derived from the gluon distribution extracted from the Q^2 evolution of $F_2(x, Q^2)$ thus represents a crucial test on the validity of the perturbative QCD framework at low x.

2　Measurement Strategy

The model independent measurement of F_L requires several sets of NC cross sections at fixed x and Q^2 but different y. This was achieved at HERA by variation of the proton beam energy.

The measurements of the NC cross sections by H1 and ZEUS are performed using e^+p data collected in 2007 with a positron beam energy $E_e = 27.5\,\text{GeV}$ and with three proton beam energies: the nominal energy $E_p = 920\,\text{GeV}$, the smallest energy of $460\,\text{GeV}$ and an intermediate energy of $575\,\text{GeV}$. The corresponding integrated luminosities are about $46\,\text{pb}^{-1}$, $12\,\text{pb}^{-1}$ and $6\,\text{pb}^{-1}$.

The sensitivity to F_L is largest at high y as its contribution to σ_r is proportional to y^2. The high reconstructed y values correspond to low values of the scattered positron energy, E'_e:

$$y = 1 - \frac{E'_e}{E_e}\sin^2(\theta_e/2) , \quad Q^2 = \frac{E_e'^2\sin^2\theta_e}{1 - y} , \quad x = Q^2/sy. \quad (2)$$

The measurement in the high y domain up to $y = 0.90$ requires the measurement of the scattered positron down to $E'_e \approx 3\,\text{GeV}$. Thus, one needs a reliable identification

and reconstruction of events with a low scattered positron energy. Furthermore, small energy depositions caused by hadronic final state particles can also lead to fake positron signals. The large size of this background, mostly due to the photoproduction process at $Q^2 \simeq 0$, makes the measurement at high y especially challenging.

2.1   H1 Analysis

H1 performed two independent analyses, at medium [8] and high [9] Q^2, with the positrons scattered into the acceptance of the backward Spacal calorimeter (the polar angle range of the scattered positron $\theta_e \gtrsim 153°$), corresponding to $12 \leq Q^2 \leq 90\,\mathrm{GeV}^2$, and into the acceptance of the Liquid Argon calorimeter (LAr) ($\theta_e \lesssim 153°$), corresponding to $35 \leq Q^2 \leq 800\,\mathrm{GeV}^2$.

The scattered positron is identified as a localised energy deposition (cluster) with energy $E'_e > 3.4(> 3)\,\mathrm{GeV}$ in the Spacal (LAr). The NC events are triggered on positron energy depositions in the Spacal or LAr calorimeters, on hadronic final state energy depositions in the Spacal, and using a new trigger hardware commissioned in 2006. At small positron energies the Spacal trigger is complemented by the central inner proportional chamber (CIP) track trigger which reduces the trigger rate to an acceptable level. The new trigger system includes the Jet Trigger, which performs a real time clustering in the LAr, and the Fast Track Trigger (FTT) [7], which utilizes on-line reconstructed tracks in the central tracker (CT). The combined trigger efficiency reaches $97 - 98\%$ at $E'_e = 3\,\mathrm{GeV}$ and $\approx 100\%$ at $E'_e > 6 - 7\,\mathrm{GeV}$.

To ensure a good reconstruction of kinematical properties, the reconstructed event vertex is required to be within 35 cm around the nominal vertex position along the beam axis. The primary vertex position is measured using tracks reconstructed in the central tracker system. The positron polar angle is determined by the positions of the interaction vertex and the positron cluster in the calorimeter.

The photoproduction background is reduced by demanding a track from the primary interaction pointing to the positron cluster with an extrapolated distance to the cluster below 6 (12) cm in the medium (high) Q^2 analysis. In the medium Q^2 analysis the fake positron background is reduced by the requirement of a small transverse size of the cluster in the Spacal, R_{log}, which is estimated using a logarithmic energy weighted cluster radius, and by the requirement that the energy behind the cluster, measured in the hadronic part of the Spacal, may not exceed 15% of E'_e. For $E'_e < 6\,\mathrm{GeV}$ in the high Q^2 analysis the following additional requirements are applied: small transverse energy weighted radius of the cluster (Ecra < 4 cm) and matching between the energy of the cluster and the track momentum ($0.7 < E'_e/P_{track} < 1.5$).

Further suppression of photoproduction background is achieved by requiring longitudinal energy-momentum conservation $\Sigma_i(E_i - p_{z,i}) > 35\,\mathrm{GeV}$, where the sum runs over the energy and longitudinal momentum component of all particles in the final state including the scattered positron. For genuine, non-radiative NC events it is

equal to $2E_e = 55\,\text{GeV}$. This requirement also suppresses events with hard initial state photon radiation. QED Compton events are excluded using a topological cut against two back-to-back energy depositions in the calorimeters.

In addition, a method of statistical background subtraction is applied for the $E_p = 460$ and $575\,\text{GeV}$ data at high y $(0.38 < y < 0.90$ and $E'_e < 18\,\text{GeV})$. The method relies on the determination of the electric charge of the positron candidate from the curvature of the associated track. Only candidates with right (positive) sign of electric charge are accepted. The photoproduction background events are about equally shared between positive and negative charges. Thus, by selecting the right charge the background is suppressed by about a factor of two. The remaining background is corrected for by statistical subtraction of background events with the wrong (negative) charge from the right sign event distributions. This subtraction procedure requires a correction for a small but non-negligible charge asymmetry in the background events due to enlarged energy depositions in the annihilation of anti-protons in the calorimeters.

The small photoproduction background for the $920\,\text{GeV}$ data at $y < 0.5(0.56)$ in the medium (high) Q^2 analysis is estimated and subtracted using a PHOJET (PYTHIA) simulation normalised to the photoproduction data tagged in the electron tagger located downstream of the positron beam at 6 m.

2.2   ZEUS Analysis

ZEUS developed special triggers to record events with low positron energy. The performance of these triggers was demonstrated in a ZEUS measurement of NC cross section at high y [10].

The scattered positron with energy $E'_e > 6\,\text{GeV}$ is identified in the ZEUS rear calorimeter at radii above ≈ 28 cm from the beam line. The standard tracking in ZEUS is limited to the particle polar angles of $\theta \lesssim 154°$. To suppress large photoproduction background caused by neutral particles (mostly photons from $\pi°$ decays) it is crucial to extend this region. A new method is used to define a corridor between the reconstructed vertex of the event and the position of the positron candidate in the calorimeter. Counting hits in the tracking detector within the corridor and comparing it to the number of the traversed layers in the tracker allows to discriminate between charged and neutral particles up to $\theta \lesssim 168°$.

The remaining background among positron candidates was estimated using the PYTHIA simulation of photoproduction events. The MC sample was normalised using the rate of identified photoproduction events with a fake positron candidate in the main detector and a signal in the electron tagger located downstream of the positron beam at 6 m.

To ensure a good reconstruction of kinematical properties and to further suppress photoproduction background, the reconstructed event vertex is required to be within

30 cm around the nominal vertex position and the measured value of $\Sigma_i(E_i - p_{z,i})$ to be between 42 and 65 GeV.
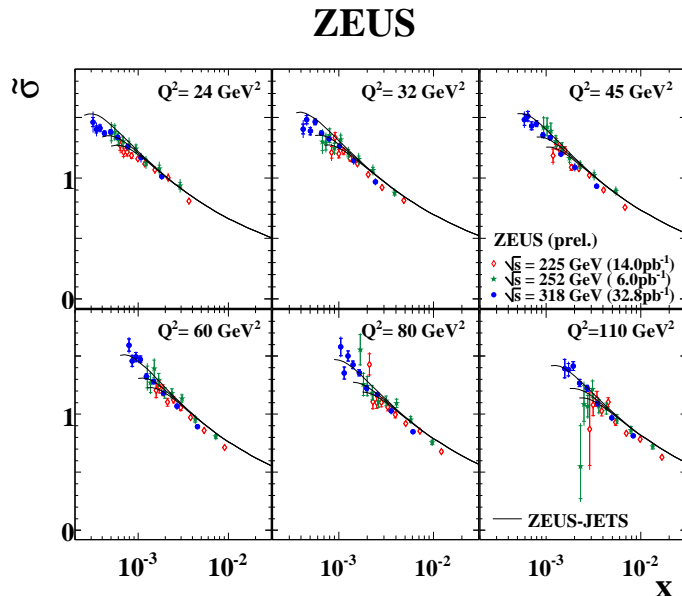
ZEUS

Figure 1: Reduced cross section measured by ZEUS at proton beam energies of 920, 575 and 460 GeV as a function of x at fixed values of Q^2.

3   HERA Results for $F_L(x, Q^2)$

The reduced NC cross sections measured by ZEUS [11] for three proton beam energies of 460, 575 and 920 GeV are shown in figure 1 as a function of x at fixed values of Q^2. They cover the range $24 \leq Q^2 \leq 110 \, \text{GeV}^2$ and $0.1 \leq y \leq 0.8$ which results in different coverage in x. The measurements are compared with the NLO QCD predictions based on the ZEUS-JETS QCD fit [12] taking into account the contribution from F_L which causes a turn over of the expected cross section at lowest x values measured.

The reduced NC cross sections measured by H1 at medium and high Q^2 ($35 \leq Q^2 \leq 800 \, \text{GeV}^2$) in the range $0.1 \leq y \leq 0.56$ for the $E_p = 920 \, \text{GeV}$ data and $0.1 \leq y \leq 0.9$ for the 460 and 575 GeV data are shown in figure 2 (left). At $Q^2 \leq 25 \, \text{GeV}^2$ ($Q^2 \geq 120 \, \text{GeV}^2$) the measurements are entirely from the medium (high) Q^2 analysis. In the intermediate Q^2 range $35 \leq Q^2 \leq 90 \, \text{GeV}^2$ the cross section is measured at $E_p = 460(920) \, \text{GeV}$ in the medium (high) Q^2 analysis and for the $E_p = 575 \, \text{GeV}$ data the cross section is obtained either using the LAr or Spacal. Small, 1-2%, relative normalisation corrections to the measured cross sections at $E_p = 460, 575$
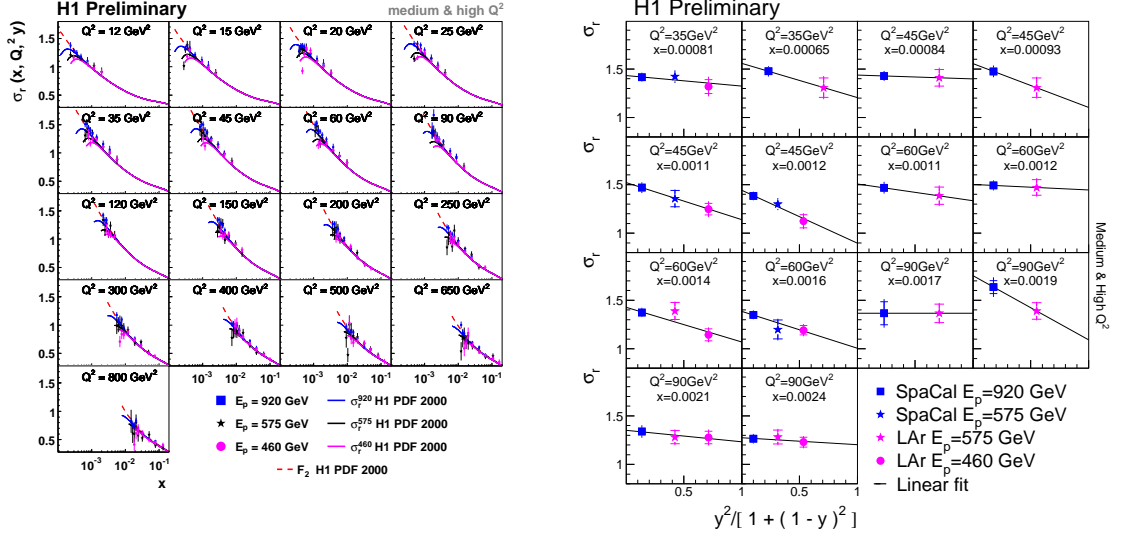
Figure 2: Reduced cross section measured by H1 at proton beam energies of 920, 575 and 460 GeV as a function of x at fixed values of Q^2 (left) and at fixed values of x and Q^2 as a function of $y^2/[1+(1-y)^2]$ for measurements which include both the LAr and Spacal data (right). The lines in the right figure show the linear fits used to determine $F_L(x, Q^2)$ for selected Q^2 and x.

and 920 GeV, common for both analyses, are derived using measurements at low y and applied to the cross section points shown in the figure. In this low y region, the cross sections are determined by $F_2(x, Q^2)$ only, apart from a small correction for residual F_L contribution.

The longitudinal structure function is extracted from the slope of the measured reduced cross section versus $y^2/[1+(1-y)^2]$. This procedure is illustrated for the H1 analysis in figure 2 (right) for selected Q^2 and x values, where both the LAr and Spacal measurements are available. The measurements are consistent with the expected linear dependence, demonstrating consistency of the two independent analyses, which utilize different detectors to measure the scattered positron.

The $F_L(x, Q^2)$ values are determined in straight-line fits to the $\sigma_r(x, Q^2, y)$. The ZEUS result for $F_L(x, Q^2)$ is shown in figure 3. The result is consistent with the expectation based on the ZEUS-JETS QCD fit [12].

The H1 measurements of $F_L(x, Q^2)$ with statistical errors better than 10% are shown in figure 4. The central $F_L(x, Q^2)$ values are determined in the fits using statistical and uncorrelated systematic errors added in quadrature, and statistical (total) F_L errors - in the fits using statistical (total) errors. The uncertainty due to the relative normalisation of the cross sections is added in quadrature to the total
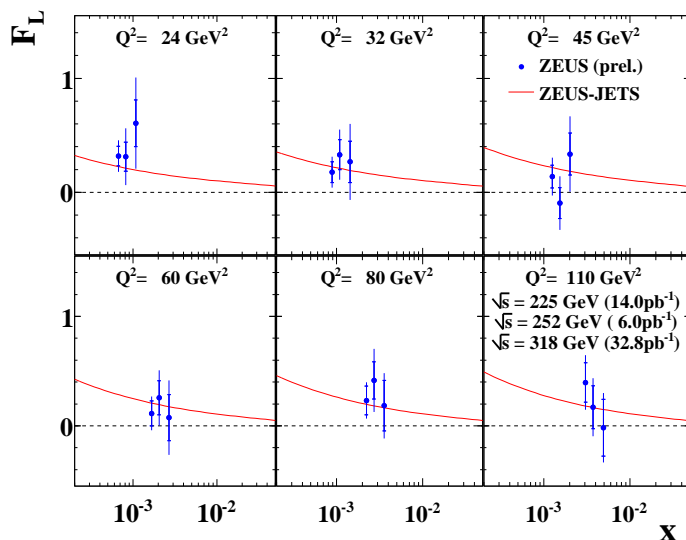
ZEUS

Figure 3: $F_L(x, Q^2)$ measured by ZEUS as a function of x at fixed values of Q^2. The inner and outer error bars are the statistical and total errors, respectively. The curve represents the NLO QCD prediction derived from the ZEUS-JETS fit to previous ZEUS data.

$F_L(x, Q^2)$ error. This uncertainty is estimated from the effect of a 1% variation of the normalisation of the $920\,\mathrm{GeV}$ cross section on the fit result. The measurement of $F_L(x, Q^2)$ is limited to Q^2 and x values where the total F_L error is below 0.4 (1.1) for $Q^2 \leq 35\ (> 35)\,\mathrm{GeV}^2$. The result is consistent with the NLO QCD prediction based on the H1 PDF 2000 fit [6] performed using previous H1 cross section data at nominal proton energy.

The H1 measurements of $F_L(Q^2)$ averaged over x at fixed Q^2 are presented in figure 5. The average is performed using the total errors of individual measurements. The overall correlated component for the averaged F_L is estimated to vary between 0.05 and 0.10. The averaged F_L is compared with the H1 PDF 2000 fit [6] and with the expectations from global parton distribution fit at NNLO (NLO) perturbation theory performed by the MSTW [2] (CTEQ [3]) group and from the NNLO QCD fit by Alekhin [4] (see also figures in [9]). Within the experimental uncertainties the data are consistent with these predictions.
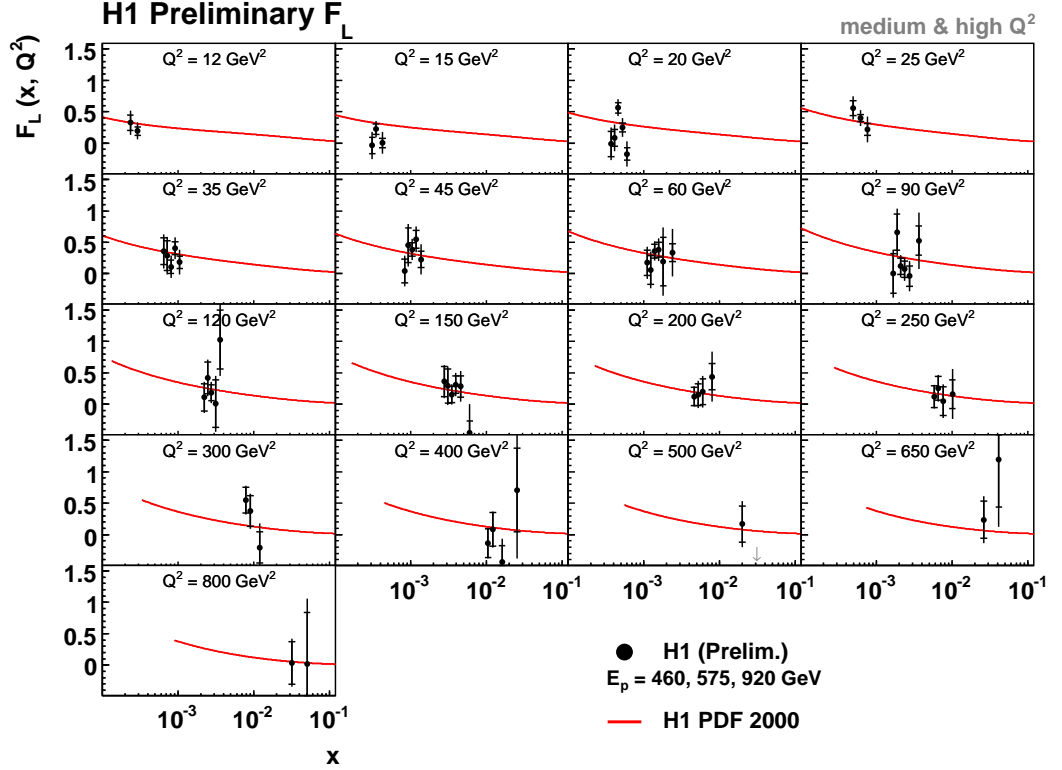
Figure 4: $F_L(x, Q^2)$ measured by H1 as a function of x at fixed values of Q^2. The inner and outer error bars are the statistical and total errors, respectively. The curve represents the NLO QCD prediction derived from the H1 PDF 2000 fit to previous H1 data.

4 Summary

The H1 and ZEUS measurements of the longitudinal proton structure function in deep inelastic scattering at low x are presented. The $F_L(x, Q^2)$ values are extracted from three sets of cross section measurements at fixed x and Q^2, but different inelasticity y obtained using three different proton beam energies at HERA. For the Q^2 range between 12 and $800 \, \text{GeV}^2$, the F_L results are consistent at the current level of accuracy with the DGLAP evolution framework of perturbative QCD at low x.
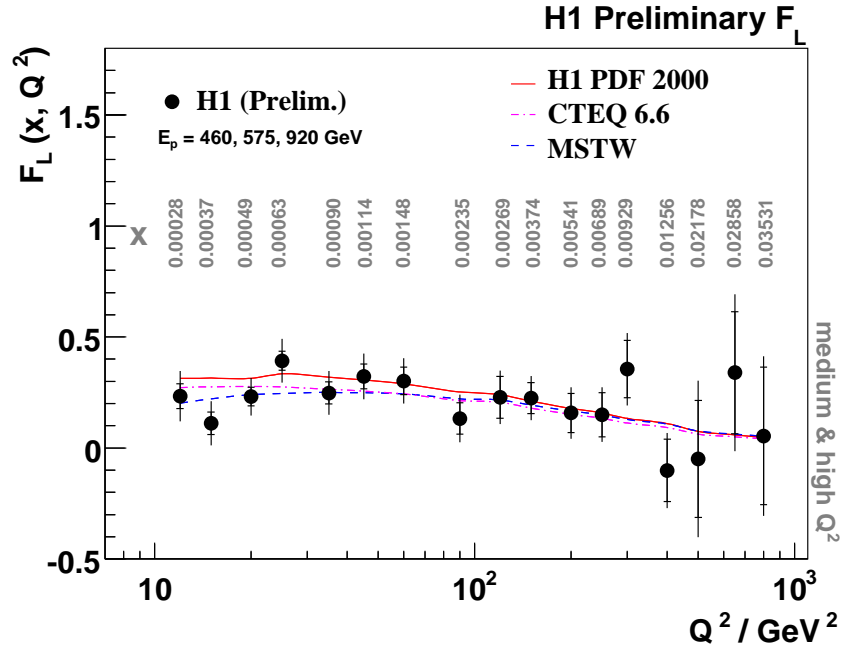
Figure 5: The H1 measurement of $F_L(Q^2)$ averaged over x at fixed values of Q^2. The resulting x values of the averaged F_L are given in the figure for each point in Q^2. The curves represent the QCD predictions.

References

[1] S. Moch, J.A.M. Vermaseren and A. Vogt, Phys. Lett. **B606** 123 (2005) and references therein.

[2] A.D. Martin, W.J. Stirling, R.S. Thorne and G. Watt, Phys. Lett. **B652** 292 (2007).

[3] J. Pumplin, H.L. Lai and W.K. Tung, Phys. Rev. **D75** 054029 (2007);
P.M. Nadolsky *et al.*, arXiv:hep-ph/0802.0007.

[4] S. Alekhin, K. Melnikov, F. Petriello, Phys. Rev. **D74** 054033 (2006).

[5] C. Adloff *et al.*, H1 Collaboration, Phys. Lett. **B393** 452 (1997);
C. Adloff *et al.*, H1 Collaboration, Eur. Phys. J. **C21** 33 (2001).

[6] C. Adloff *et al.*, H1 Collaboration, Eur. Phys. J. **C30** 1 (2003).

[7] A. Baird *et al.*, IEEE Trans. Nucl. Sci. **48** 1276 (2001).

[8] A. Nikiforov, *Measurement of the Proton F_L and F_2 Structure Functions at Low x*, 43rd Rencontres de Moriond on QCD and High Energy Interactions, La Thuile, Aosta Valley, Italy (8-15 March 2008);
B. Antunovic, *Measurement of the Longitudinal Structure Function F_L at Low x in the H1 Experiment at HERA*, 16th International Workshop on Deep Inelastic Scattering, London (7-11 April 2008);
F.D. Aaron *et al.*, H1 Collaboration, Phys. Lett. **B665** 139 (2008).

[9] V. Chekelian, *Direct F_L Measurement at High Q^2 at HERA*, 16th International Workshop on Deep Inelastic Scattering, London (7-11 April 2008);
H1 Collaboration, H1prelim-08-042,
`http://www-h1.desy.de/h1/www/publications/htmlsplit/H1prelim-08-042.long.html`

[10] S. Shimizu, *ZEUS High-y Cross Section Measurement and Preparation for Low Energy Running*, Proceedings of the 15th International Workshop on Deep-Inelastic Scattering and Related Subjects, ed. G. Grindhammer and K. Sachs, Verlag Deutsches Elektronen-Synchrotron, April 2007, Munich, Germany, p.289.

[11] D. Kollár, *Measurement of the Longitudinal Structure Function F_L at Low x at HERA with the ZEUS Detector*, 16th International Workshop on Deep Inelastic Scattering, London (7-11 April 2008);
ZEUS Collaboration, ZEUS-prel-08-001,
`http://www-zeus.desy.de/public_results/publicsearch.html`,
search-key: ZEUS-prel-08-001.

[12] S. Chekanov *et al.*, ZEUS Collaboration, Eur. Phys. J. **C42** 1 (2005).